Failure Analysis of Rubber Toughened Epoxy Resin

Vineeta Nigam, D. K. Setua, G. N. Mathur

Defence Materials & Stores Research & Development Establishment, G. T. Road, Kanpur – 208013, India

Received 28 June 2001; accepted 14 May 2002

ABSTRACT: Failure of the blends of epoxy cresol novolac resin (ECN) with varied proportions of carboxy terminated polybutadiene (CTPB) liquid functional rubber was studied. Addition of CTPB improves toughness as reflected in the improvement of tensile, flexural, and impact properties. However, 10 wt % of CTPB was the optimum concentration beyond which a rapid fall of properties, in all cases, was observed. Surface topography of the fractured surfaces, studied by scanning electron microscopy and atomic force microscopy, revealed marked changes in the phase morphology due to addition of rubber and also accounted for the variation of the strength properties. © 2002 Wiley Periodicals, Inc. J Appl Polym Sci 87: 861–868, 2003

Key words: resins; rubber; atomic force microscopy (AFM)

INTRODUCTION

Brittle epoxy resins are generally toughened by the addition of liquid functional rubbers [e.g., carboxy-terminated polybutadiene (CTPB)] and copolymers of amino-terminated butadiene and acrylonitrile (ATBN) and carboxy-terminated butadiene and acrylonitrile (CTBN).[1, 2] Even a small quantity of such rubbers can cause significant changes in the toughness characteristics. These changes are reflected by a marked increase in the mechanical properties, such as tensile, flexural, or impact strengths.[1–4] McGarry and Wilson[5] and Sultan et al.[6]reported an increase of the fracture toughness properties of diglycidyl ether of bisphenol A (DGEBA) by addition of liquid CTBN. There have been few similar reports on rubber-modified epoxy resins.[7–10]

At a volume fraction of 5–30 wt % of rubber into epoxy resin, Guild and Kinloch[11] reported the presence of dispersed rubber particles with an average size 0.5–5 μm. The presence of these particles was also observed to increase the toughness without significantly decreasing other important properties. Despite the volume fraction, the dispersed rubber particles acted as stress absorbers and assisted in the deflection or arresting of the growing cracks during failure. However, the failure resistance efficacy of the blends depends on the rubber concentration, particle size, homogeneity of dispersion, and interfacial adhesion between the particles with the matrix.[12–14] Variation in the rubber and epoxy concentrations also govern the characteristics of phase morphology and failure properties.[15–21] Qian et al.[22] utilized scanning electron microscopy (SEM) and transmission electron microscopy (TEM) to interpret the particle–epoxy interface characteristics. Yamanaka and Inoue[23] reported the phase separation mechanism during the cure reaction of DGEBA and CTBN by light scattering, microscopy, torsional braid analysis, and differential scanning calorimetry (DSC). Hwang et al.[24] studied the morphology of fatigue crack propagation of rubber-toughened epoxies. Setua et al.[25–28] have reported SEM and AFM studies on the phase morphology and failure mechanism of rubber blends and composites. In these cases, attempts were made to correlate the relative strength of different vulcanizates with the features of the failure surfaces. We have recently reported our studies on the cure characterization, dynamic mechanical analysis, physicomechanical properties, phase morphology development, and wide-angle X-ray scattering (WAXS) studies of epoxy cresol novolac resin (ECN)–CTPB[29, 30] and ECN–CTBN[31, 32] blends.

In the present paper we attempt to correlate the tensile, flexural, and impact properties of CTPB-modified ECN with the SEM and AFM photographs of the mechanically fractured surfaces.

EXPERIMENTAL

ECN resin was synthesized in the laboratory by heating novolac and epichlorohydrin in fixed proportion (weight ratio 1:8) at 120°C in the presence of 40% methanolic sodium hydroxide solution as catalyst. CTPB was obtained from trade (grade, Hycar CT-RLP, 2000x162). The characteristic properties of ECN (as determined in the laboratory) and CTPB (taken from the trade literature) are shown in Tables I and II,

Correspondence to: D. K. Setua (dmsrde@sancharnet.in).

Journal of Applied Polymer Science, Vol. 87, 861–868 (2003)

TABLE I
Typical Properties of Epoxy Cresol Novolac Resin (ECN)

Property	Value
Molecular weight (Mn)	850
Softening point (°C)	40–45
Epoxy equivalent weight (gm/mole)	220
Physical state	Viscous fluid

respectively. Composition of the blends with varied ECN and CTPB content along with the requisite amount of diamino diphenyl methane (DDM) as curing agent are appended in Table III. To a preheated and mechanically stirred ECN at 70°C, CTPB was mixed for 0.5 h, followed by the addition of DDM. The mixing was continued until complete dissolution of DDM. An iron mold was pretreated with silicon oil at 200°C for 2 h and then cooled to room temperature (25 $\pm$ 2°C) to cover the iron surface with a uniform silicon film. The mold was then stabilized at 150°C in the oven. The blend was then poured into the mold with the help of a muslin cloth to minimize formation of air bubbles in the castings. Curing was carried out in the mold for 2 h at 150°C, and the sample was further post cured at 200°C for 2 h.

Tensile test was carried out with samples of size 160 $\times$ 16 $\times$ 5 mm in a Universal testing machine (UTM) at a crosshead speed of 3 mm/min as per ASTM method D3039-76, and the standard deviation of strength for five samples was recorded. Similarly the flexural test (sample size: 120 $\times$ 12 $\times$ 5mm) was done in the UTM at a crosshead speed of 32 mm/min as per ASTM method D790-81, and standard deviation was calculated. Charpy impact testing was carried out at room temperature in a Tinius Olsen computer-controlled model 8000 A UTM with a hammer mass of 15 kg, which was deflected at a 90° angle from the vertical and allowed to fall and strike the samples. The striking energy applied on the sample (size, 7.5 $\times$ 12 $\times$ 4 mm) was 70.20 J.

The fractured surfaces were cleaned with an air blower to remove the dust particles and were then sputter coated with gold without touching the surface. The gold-coated samples were subsequently studied by SEM (Model JSM 35 CF, Scanning Electron Microscope) for morphological information.

TABLE II
Typical properties of Carboxy Terminated Polybutadiene (CTPB)

Property	Value
Molecular weight (M_n)	3500
Brookfield viscosity, mPa (27°C)	125000
Carboxyl content (%)	2.37
Specific gravity at 27°C (g/cm^3)	0.948
Acrylonitrile content (%)	17
Functionality (%)	1.85

TABLE III
Formulation of ECN and CTPB Blends Containing DDM

Nomenclature of the Blends[a]	ECN (g)	CTPB (g)	DDM (g)
ER_0	100	0	23.0
ER_5	95	5	21.5
ER_{10}	90	10	20.0
ER_{15}	85	15	19.2
ER_{25}	75	25	17.1

[a] Number in the subscript of *R* stands for wt % of rubber into the blends.

AFM studies on the fractured surfaces of the test specimen failed under tensile testing were investigated in a Digital Instrument's (USA) model Nanoscope, in the intermittent contact mode. Contrast in phase images comes primarily from three factors: surface topography, differences in adhesion between the tip and sample, and differences in the elastic modulus of the sample. Phase is often used to distinguish different components within a material and to highlight topographical details. The images were acquired using an ultra lever silicon cantilever and probe. For the samples that were analyzed, an image of the cross section was taken.

RESULTS AND DISCUSSION

Tensile, flexural, and impact strengths of the neat resin (ER_0) as well as rubber–epoxy blends (e.g., ER_5, ER_{10}, ER_{15}, and ER_{25}) along with the standard deviations are depicted in Figures 1–3. Tensile strength of the blends is increased due to addition of CTPB up to 10 wt %, beyond which it falls. At 10 wt % of the rubber, the matrix is sufficiently restrained and the propagation of the fracture fronts during failure is hindered. Further, the chemical interaction between the rubber and the epoxy resin lead to interphase coupling. However, at a concentration of rubber exceeding 10 wt %, inhomogeneous dispersion of the rubbery phase occurred due to coalescence of the rubber particles. Cheng et al.[33] proposed that the addition of a rubbery phase introduces a cavitational mechanism that relieve the hydrostatic strain energy and enhances the shear yielding of the matrix. The tensile strength, therefore, drops beyond a 10 wt % loading of the CTPB.

A SEM photograph of the phase morphology of the tensile fractured surface of the neat epoxy resin is shown in Figure 4. The parabolic or clam-shaped fracture evident in this figure indicates brittle failure.[30] Addition of 5 wt % of CTPB into the epoxy resin did not cause any major change in the morphology. This effect is probably due to an insufficient rubber content

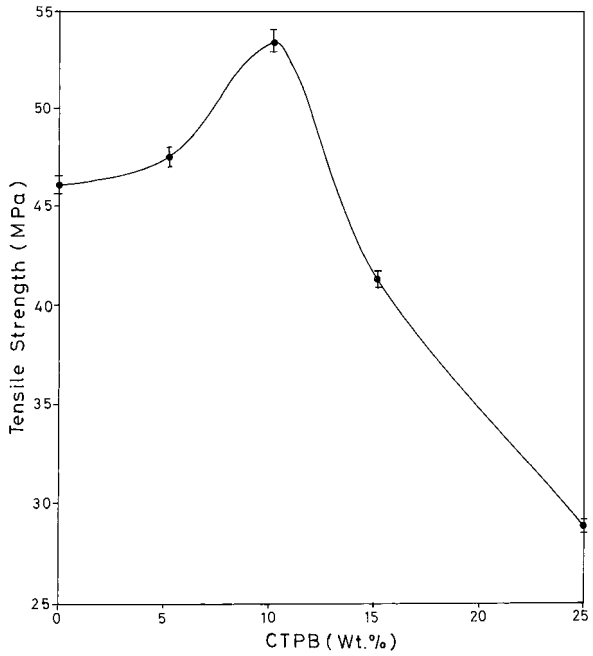

Figure 1 Plot of tensile strength versus CTPB concentration.

into the matrix resin. However, the presence of CTPB as the dispersed rubber and efficient stress transfer across the interface caused a net increase of the tensile strength property (Figure1). The SEM photograph of the tensile fractured surface of the blend containing 10 wt % rubber (ER_{10}), shown in Figure 5, indicates occasional stopping of the fracture fronts by the presence of cavities due to ejected rubber particles, as proposed by Cheng et al.[33] Increasing rubber concentrations either at 15 wt % or further to 25 wt % caused the dispersed particles to grow larger and larger due to rubber phase coalescence.[32] The SEM photograph (Figure 6) of the 25 wt % CTPB blend (ER_{25}) shows the occluded epoxy phase into the grown rubber particles. Reduced restriction to the propagation of the fracture fronts due to increase in the mean diameter of the rubbery phase as well as their inhomogeneous distribution might be the cause of an inferior elastic recovery, lower hysteresis, and poor tensile properties.

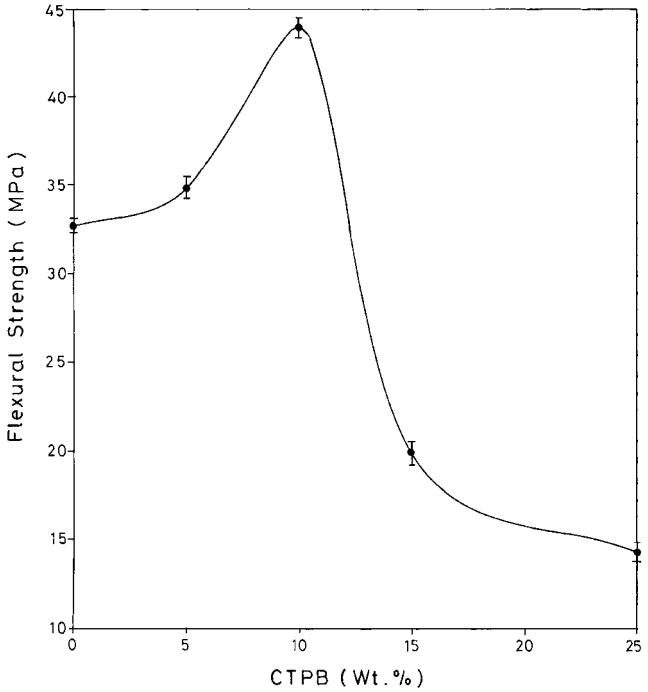

Figure 2 Plot of flexural strength versus CTPB concentration.

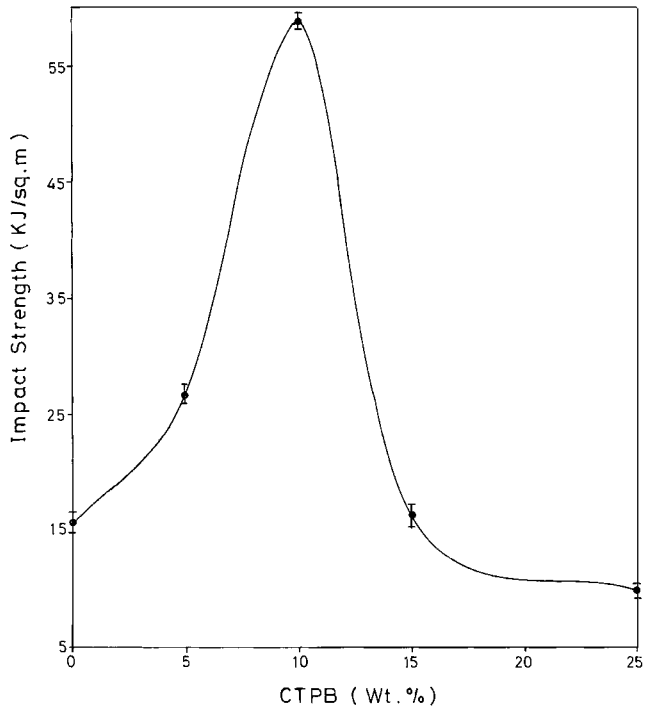

Figure 3 Plot of impact strength versus CTPB concentration.

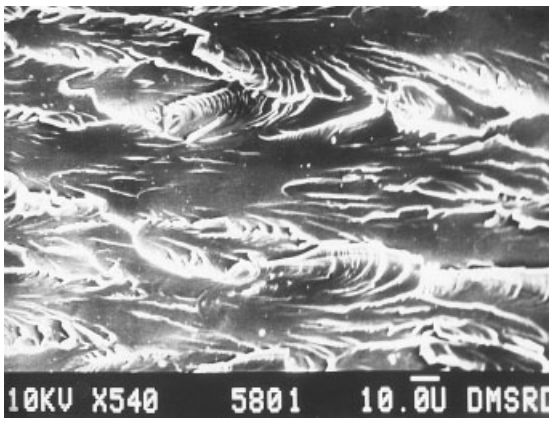

Figure 4 SEM photomicrograph of tensile fractured surface of neat epoxy resin.

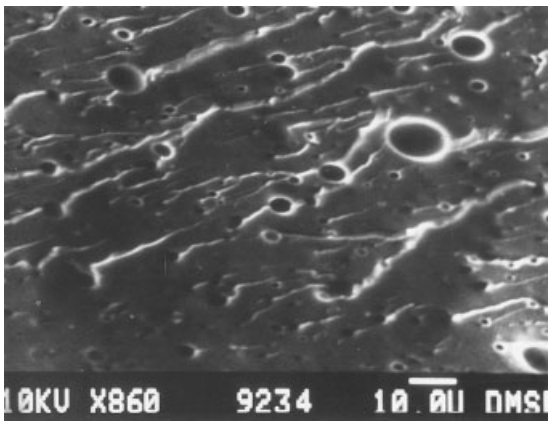

Figure 5 SEM photomicrograph of tensile fractured surface of ECN–CTPB blend with 10 wt % CTPB.

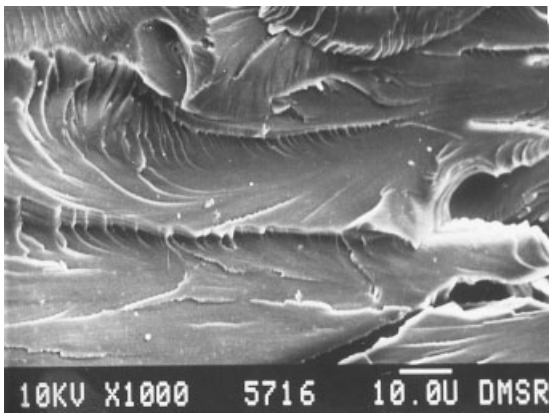

Figure 7 SEM photomicrograph of flex fractured surface of neat epoxy resin.

As already discussed, the enhancement of strength properties depends on the extent of rubber–epoxy adhesion. This dependence is envisaged through the chemical interaction between the carboxyl group of CTPB with the oxirane group of epoxy resin to form ester linkages. Fourier transform infrared (FTIR) studies to confirm the latter have already been reported.[30] Neat epoxy resin shows characteristic peaks at 860 and 910 cm^{-1} due to presence of its oxirane group, whereas CTPB shows peaks at 1310, 1420, 1700–1730, and 1825 cm^{-1} for the carboxyl group. Esterification between oxirane and carboxyl groups resulted in formation of newly stretched peaks in the regions 1550–1610 and 1300–1400 cm^{-1} and disappearance of the peak at 1700–1730 cm^{-1}. Increasing rubber content beyond 10 wt %, caused phase growth due to rubber coalescence and resulted in a reduced efficacy of the rubber–epoxy adhesion.

Similar to the tensile strength, rise in the flexural strength up to 10 wt % CTPB may be attributed to effective stress transfer and proper adhesion between the dispersed phase with the resin matrix. Intimate contact between the two phases also enhances the stored energy density and a corresponding improvement in the failure properties. The SEM photograph (Figure 7) of the flex-failed surface of the neat resin (ER_0) showed the occurrence of both shear deformation and crazing. The fracture pattern altogether changes when rubber is incorporated. The SEM photograph (Figure 8) of the resin containing 10 wt % CTPB (ER_{10}) has a number of fracture lines and also shows formation of cavities due to pulling out of the rubber phase from the matrix. Propagation of the fracture paths was obstructed by the presence of rubber particles. All these effects caused improvement of the flexural strength up to 10 wt % of rubber. Fracture lines are the thin hair-line fracture fronts visible on the surface that are generally originated and terminated in the middle of the fracture surface or sometimes stopped by the rubber globules. But the fracture paths are broad and spread over the entire fracture surface. They are particularly responsible for gross failure of the sample subjected to a particular mode of failure testing. Beyond a 10 wt % concentration, epoxy oc-

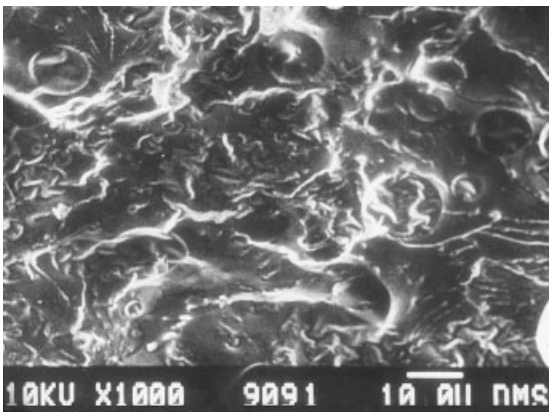

Figure 6 SEM photomicrograph of tensile fractured surface of ECN–CTPB blend with 25 wt % CTPB.

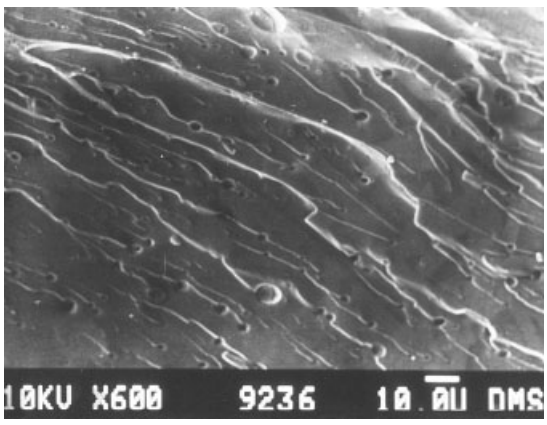

Figure 8 SEM photomicrograph of flex fractured surface of ECN–CTPB blend with 10 wt % CTPB.

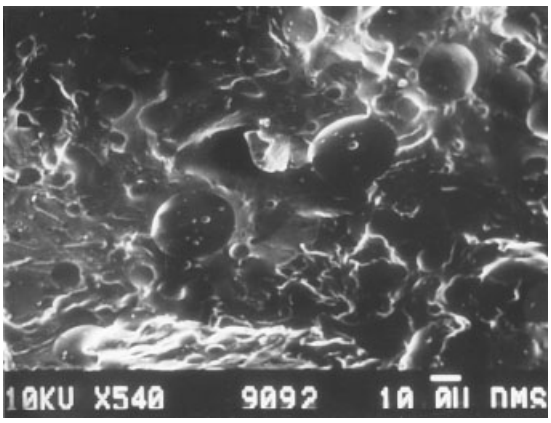

Figure 9 SEM photomicrograph of flex fractured surface of ECN–CTPB blend with 25 wt % CTPB.

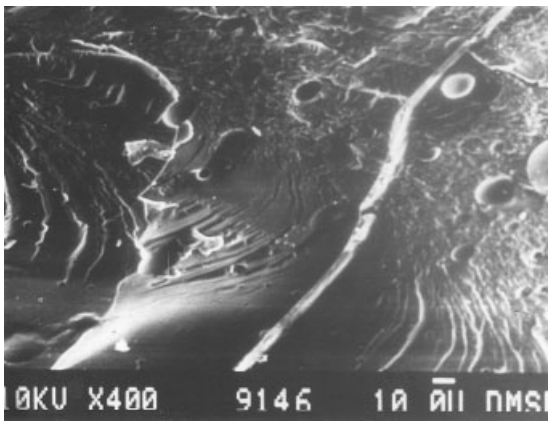

Figure 11 SEM photomicrograph of impact fractured surface of ECN–CTPB blend with 5 wt % CTPB.

cluded into the rubber phase and the extent of this occlusion increased with the increasing rubber concentration. The flex-failed morphology at 25 wt % CTPB (ER_{25}) is shown in Figure 9. An altered failure mode, absence of straight fracture paths, as well as substantial growth of the rubber phase encapsulating epoxy phase were observed. Improperly distributed and relatively short fracture lines compared with 10 wt % CTPB (Figure 8) are also present. Failure morphology, therefore, supports the resultant fall of the flexural strength at 15 or 25 wt % of CTPB.

Enhanced impact resistance of the rubber-modified epoxies resulted from a greater energy absorbing process. In the unmodified system (ER_0), shear yielding and also the formation of shear lips were observed (Figure 10). The SEM photograph (Figure 11) of the impact failed surface with 5 wt % CTPB showed formation of plastic zone as well as rubber particles resisting growth of the fracture. In the case of 10 wt % CTPB, impact properties improved remarkably due to termination of the straight fracture fronts at the matrix resin–rubber particle interface (Figure 12). At a still higher rubber content (15 wt %), the applied impact load caused the fracture of the dispersed phase boundaries (Figure 13). The fracture topography in Figure 13 also shows the formation of a layered structure, which might be due to failure in separate planes. All these factors ,such as rubber concentration and particle size as well as rubber–epoxy adhesion, caused significant variation in the toughness characteristics of the blends and are collectively responsible for an abrupt fall in the impact properties beyond a 10 wt % loading of CTPB.

AFM STUDIES

To further emphasize the SEM observations, AFM analysis of the tensile fractured surfaces of the blends were carried out. The AFM image of the blend with 10 wt % CTPB (ER_{10}) is shown in Figure 14.The presence of spherical rubber globules of different dimensions (0.2–1.5 μm) on the surface of epoxy resin matrix as well as stoppage of the propagation of fracture fronts are clearly evident. These rubber particles are subse-

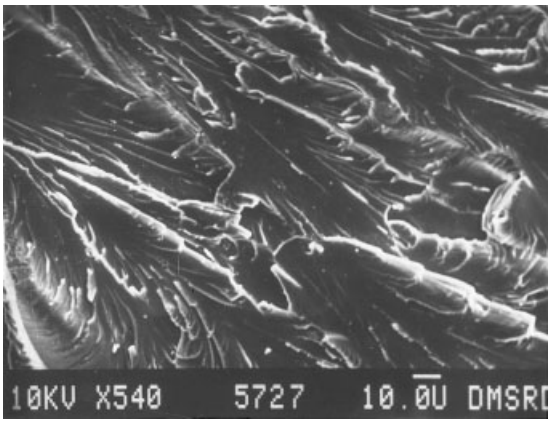

Figure 10 SEM photomicrograph of impact fractured surface of neat epoxy resin.

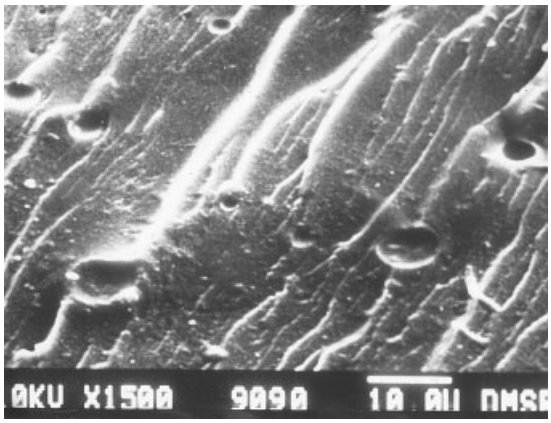

Figure 12 SEM photomicrograph of impact fractured surface of the ECN–CTPB blend with 10 wt % CTPB.

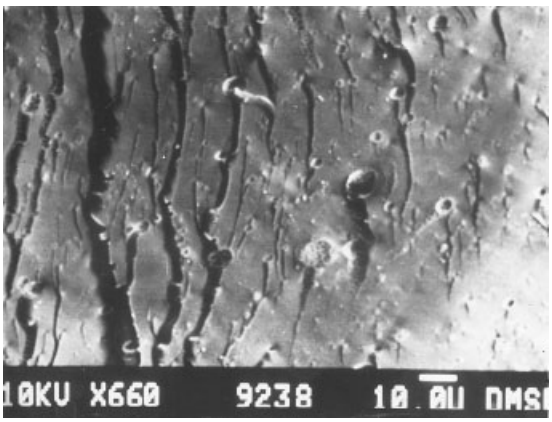

Figure 13 SEM photomicrograph of impact fractured surface of the ECN–CTPB blend with 15 wt % CTPB.

quently pulled out and form cavities, as shown in SEM photograph in Figure 5. That the resin matrix has sufficiently interlinked at the rubber particle surface though chemical interaction is shown in another AFM image (Figure 15) of this blend at higher magnification (scan size, 20.08 μm; scan rate, 0.5003 Hz). The rubber particle was observed to be embedded in a fibrous surface of epoxy, and the fibers also tended to bend in towards the interface. Probably this type of close association between the matrix with the dispersed particle enhanced the strength properties at 10 wt % of rubber.

The AFM image of a blend with 25 wt % CTPB (ER_{25}) is shown in Figure 16. Growth of the rubber phase due to phase coalescence, fibrous structure of the matrix, and cracks on the surface are the characteristic features of the fracture surface. The intermediate stage of occlusion of epoxy into the rubber phase is shown in AFM images of this blend in Figure 17 and also at a higher magnification in Figure 18.

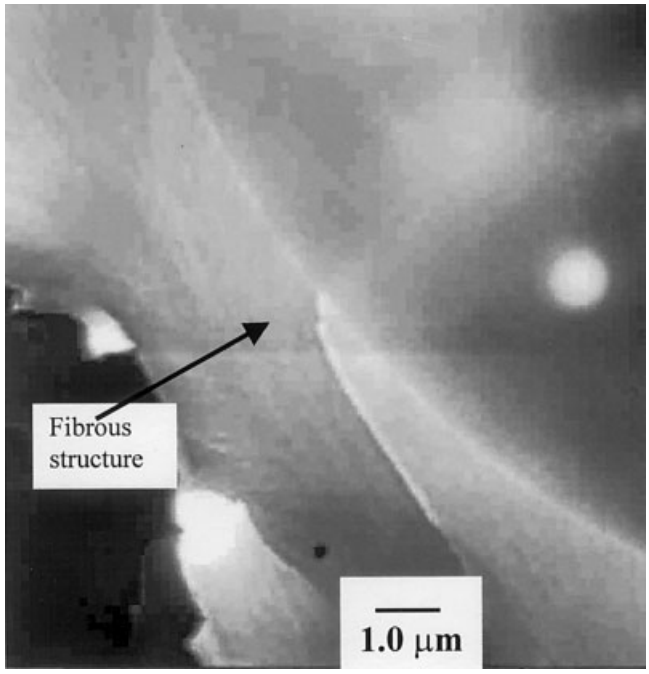

Figure 15 AFM image of tensile fractured surface of ECN–CTPB blend at higher magnification with 10 wt % CTPB.

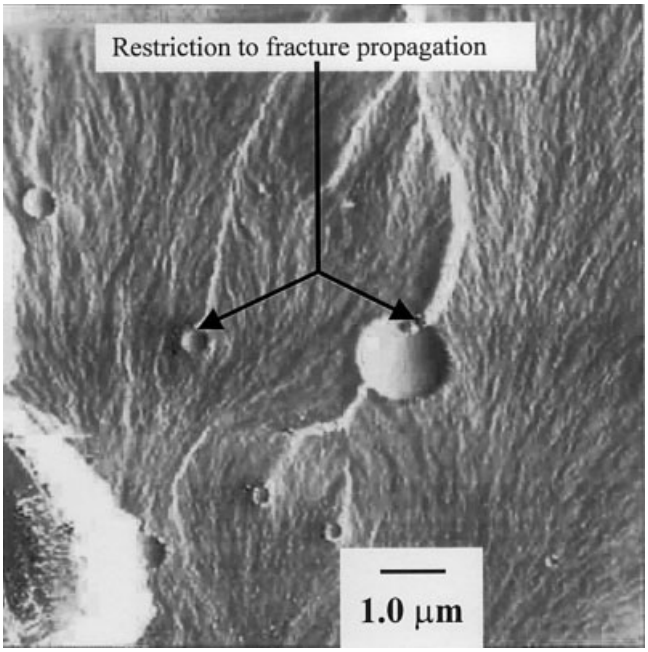

Figure 14 AFM image of tensile fractured surface of ECN–CTPB blend with 10 wt % CTPB.

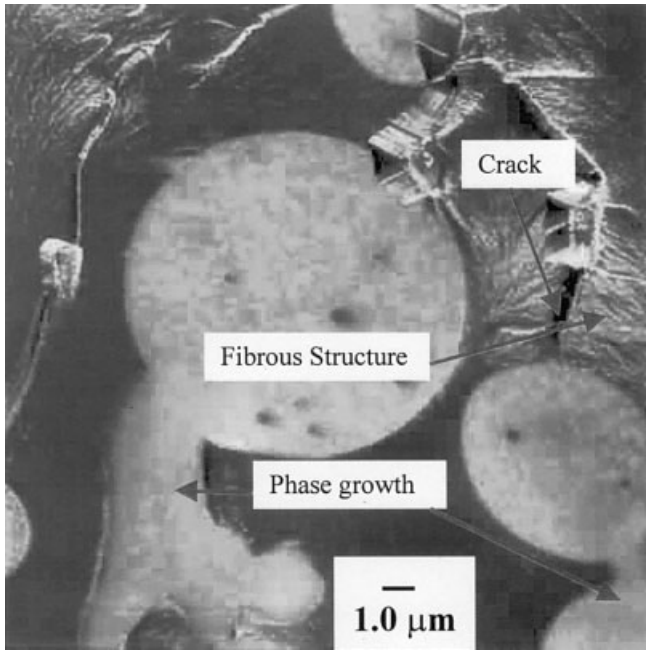

Figure 16 AFM image of tensile fractured surface of ECN–CTPB blend with 25 wt % CTPB.

CONCLUSIONS

1. CTPB at 10 wt % produced maximum benefit in the toughening of epoxy thermoset as reflected in the tensile, flexural, and impact properties.
2. SEM studies on the fracture surface topography of the blends under different test conditions provided insight; that is, formation of a two-phase system with rubber globules in the dispersed phase and ECN as the matrix; phase growth with increasing rubber concentration beyond 10 wt %; rubber–epoxy adhesion and occlusion; and cavitation due to pulling out of the rubber phase during fracture. All these features closely resemble the observed mechanical properties of the blends.
3. AFM observations closely corroborate SEM features on the chemical interaction between rubber and epoxy phases, phase morphology, and failure mechanism. AFM, with its inherent capability to produce better resolution than SEM, can offer a topographic picture of the fiber–matrix interface with fibrous structure not obtainable through SEM. Furthermore, with AFM we see hindrance to propagation of a fracture path by actual rubber particles, whereas in SEM we see that phenomenon through ejected rubber particles as cavities. The distribution and scale of the rubber particles in the matrix as well as the process of the phase growth by rubber particle coalescence are more clearly evident with AFM than SEM.

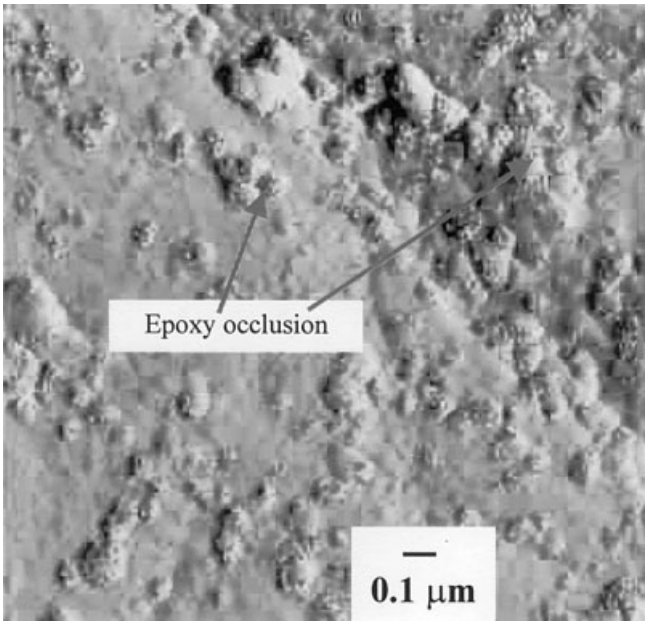

Figure 17 AFM image of tensile fractured surface of ECN–CTPB blend with 25 wt % CTPB.

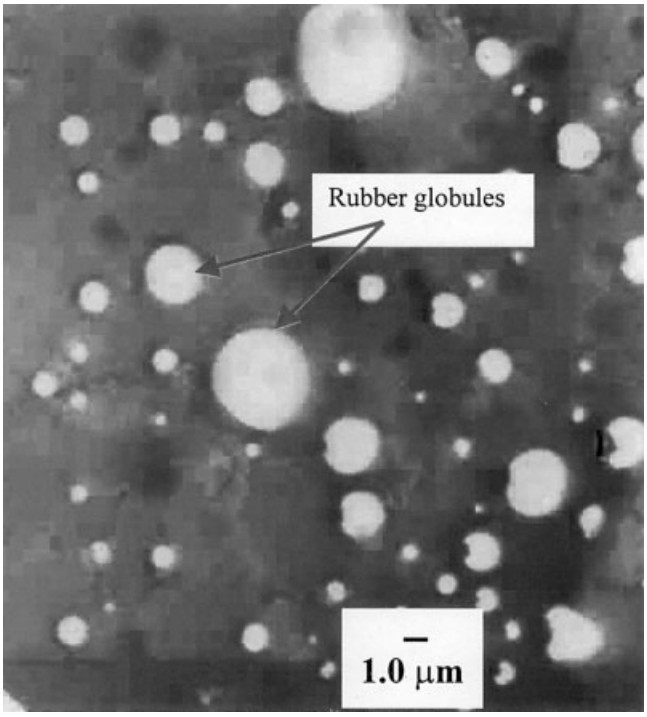

Figure 18 AFM image of tensile fractured surface of ECN–CTPB blend at higher magnification with 25 wt % CTPB.

References

1. Sultan, J.N.; Liable, R.C. McGarry, F.J. Polym Sym 1971, 16, 127.
2. Sultan, J.N.; Liable, R.C.; McGarry, F.J. Polym Eng Sci 1973, 13, 29.
3. Bascom, W.D.; Cottington, R.L.; Jones, R.L.; Peyser, P. J Appl Polym Sci 1975, 19, 2425.
4. Kunz-Douglass, S.; Beaumont, P.W.R.; Ashby, M.F. J Mater Sci 1980, 15, 1109.
5. McGarry, F.J.; Willner, A.M. Research Report, School of Engineering MIT Cambridge, MA, 1966.
6. Sultan, J.N.; Liable, R.C.; McGarry, F.J. Appl Polym Symp 1971, 16, 127.
7. Kunz, S.; Beaumont,P.W.R.; Ashby, M.F. J Mater Sci 1980, 15, 1109.
8. Kunz, S.C.; Beaumont, P.W.R. J Mater Sci 1981, 16, 3141.
9. Bucknall, C.K.; Yoshii, Y. Br Polym J 1978, 10, 53.
10. Chen, T.K.; Jan, Y.H. Polym Eng Sci 1995, 9, 778.
11. Guild, F.J.; Kinloch, A.J. J Mater Sci 1995, 30, 1689.
12. Bucknall, C.B. Toughened Plastics; Applied Science: London, 1977; p. 4.
13. Garg, A.C.; Mai, Y.W. Compos Sci Technol 1988, 31, 179.
14. Kozii, V.V.; Rozenberg, B.A. Polym Sci 1992, 34.
15. Borggreve, R.J.M.; Gaymans, R.J. Polymer 1988, 29, 144.
16. Yamanaka, K.; Takagi, Y.; Inoue, T. Polymer 1989, 30, 1839.
17. Hsich, H.S.Y. Polym Eng Sci 1990, 30, 493.
18. Yee, A.F.; Pearson, R.A. J Mater Sci 1986, 21, 2462.
19. Bagheri, R.; Pearson, R.A. J Appl Polym Sci 1995, 58, 427.
20. Bagheri, R.; Pearson, R.A. J Mater Sci 1996, 31, 3945.
21. Verchere, F.; Pascault, J.P.; Sautereau, H.; Moschiar, S.M.; Riccardi, C.C.; Williams, R.J.J. J Appl Polym Sci 1991, 42, 701.
22. Qian, J.Y.; Pearson, R.A.; Dimonie, V.L.; El-Aasser, M.L.S. J Appl Polym Sci 1995, 58, 439.
23. Yamanaka, K.; Inoue, T. J Mater Sci 1990, 25, 241.

24. Hwang, J.F.; Manson, J.A.; Hertzberg, R.W.; Miller, G.A.; Sperling, L.H. Polym Eng Sci 19989, 29, 1477.
25. Setua, D.K.; Pandey, K.N.; Saxena, A.K.; Mathur, G.N. J Appl Polym Sci 1999, 74, 480.
26. Setua, D.K.; Shukla, M.K.; Nigam, V.; Singh, H.; Mathur, G.N. Polym Comp 2000, 21, 988.
27. Setua, D.K.; Pandey, A.K.; Debnath, K.K.; Mathur, G.N. Kautschuk Gummi Kunststoffe 1999, 52(7–8), 486.
28. Nigam, V.; Setua, D.K.; Mathur, G.N. J Mater Sci 2001, 36, 43.
29. Nigam, V.; Setua, D.K.; Mathur, G.N. J Therm Anal Cal 2001, 64, 521.
30. Nigam, V.; Setua, D.K.; Mathur, G.N. J Appl Polym Sci 1998, 70(3), 537.
31. Nigam, V.; Setua, D.K.; Mathur, G.N. Polym Eng Sci 1999, 39, 1425.
32. Nigam, V.; Setua, D.K.; Mathur, G.N. Rubb Chem Technol 2000, 73, 830.
33. Cheng, C.; Hiltner, A.; Baer, E.; Soskey, P.R.; Mylonakis, S.G. J Appl Polym Sci 1994, 52, 177.